Parasitic exploitation of WiFi signals for indoor radar surveillance

Debora Pastina, *Member, IEEE*, Fabiola Colone, *Member, IEEE*, Tatiana Martelli and Paolo Falcone

Abstract—In this paper we examine the potentiality of passive coherent location (PCL) for indoor area monitoring. In particular we show that WiFi transmissions can be successfully exploited as waveforms of opportunity to perform moving target detection and localization based on the passive radar principle. Moreover, we investigate the advanced capability to obtain high resolution cross-range profiles of the observed targets via Inverse Synthetic Aperture Radar (ISAR) techniques. To these purposes, appropriate processing techniques are introduced to cope with the limitations resulting from the indoor application such as the strong returns from the stationary scene and the high density of potential targets. The proposed system concept has been tested against both simulated and real data sets. The reported results clearly show that using few receiving channels connected to properly dislocated antennas allows an accurate target localization and tracking. In addition reliable and stable profiles are obtained for the targets moving in the surveyed scene which might fruitfully feed a classification stage. This contributes to demonstrate the effective applicability of the passive radar concept for improving internal and external security of private/public premises.

Index Terms—inverse synthetic aperture radar (ISAR), disturbance cancellation, passive coherent location (PCL), passive radar, WiFi transmissions.

I. INTRODUCTION

IN recent years, there has been a growing interest in indoor localization and tracking systems due to the security and public safety issues as well as service matters. Real-world applications include, for example, people location and navigation along buildings, automotive safety, vehicle navigation or asset tracking.

Various wireless technologies have been used for indoor localization among which infrared, IEEE 802.11 wireless LAN and ultrasonic. More recently Radio Frequency Identification (RFID) has become a very attractive solution thanks to a number of desirable features, such as contactless communications, high data rate and security, non line-of-sight readability, compactness and low cost [1]-[3]. In particular, a very promising wireless technique for next generation RFID is the Ultra-Wide Bandwidth (UWB) technology because it is able to overcome most of the limitations of current narrow bandwidth RFID technology [4].

Despite the effectiveness of these techniques has been largely demonstrated, they have a major drawback. Basically, with the exception of the infrared, which however requires direct line-of-sight and is a short-range signal transmission, the above mentioned technologies require the target objects to be equipped with a cooperative device (e.g. a wireless LAN system, a RFID tag, etc.). As a consequence they are not suited for specific surveillance applications such as intruder location, detection, tracking and identification of unauthorized vehicles in a forbidden area, and so on.

Therefore, the above mentioned techniques could be nicely complemented by sensors able to operate against non-cooperative targets. To this purpose, a suitable low-cost solution is offered by the passive radar concept.

Passive coherent location (PCL) exploits existing illuminators of opportunity to perform target detection and localization thus embracing the current trend of using standard, low-cost, and already deployed technologies. PCL has been mostly investigated for long or medium range applications by exploiting the proliferation of RF systems for telecommunications [5]-[6].

Aiming at indoor surveillance or at monitoring small external areas, the IEEE 802.11 standards-based (WiFi) technology has been considered as potential source of opportunity since it offers reasonable bandwidth (range resolution), coverage and wide accessibility [7]-[8].

The possibility to exploit such a ubiquitous and easily accessible source has been shown to be an appropriate choice for the detection and localization of designated vehicles, human beings or man-made objects within short ranges using the passive radar principle [9]-[10]. In addition, the feasibility of uncooperatively and covertly detecting people moving behind walls has been investigated in [11].

As previously mentioned, the PCL sensor capabilities can be significantly enhanced if the conceived system operates in conjunction with other active/passive sensors. As a specific

D. Pastina, F. Colone, and T. Martelli are with the DIET Department, University of Rome "La Sapienza," 00184 Rome, Italy (e-mail: pastina@diet.uniroma1.it; colone@diet.uniroma1.it; martelli@diet.uniroma1.it).

P. Falcone was with the DIET Department, University of Rome "La Sapienza," 00184 Rome, Italy. He is now with ARESYS srl, 20134 Milan, Italy (e-mail: paolof1983@gmail.com).

example of this type of application, the effectiveness of the WiFi-based PCL sensor is studied by the authors as part of two projects funded by the EU under the 7th Framework Program [12]-[13]. These projects present an innovative approach to the challenging tasks required by the airport security system where the WiFi-based PCL sensor is jointly employed with other active and passive radar sensors to enhance the security level in the airport terminal area.

Among the very nice features of the PCL approach is that no extra signal is transmitted; this limits the energy consumption, prevents possible interferences with pre-existing systems, and makes the sensor free from any issue related to human health. Moreover this technique removes the requirements for cooperative targets and it is not subject to the blind spots and potentially intrusive equipment necessary for video surveillance. Therefore it could be used in public areas (railways, airports, etc.) or private commercial premises such as office buildings or warehouses.

The main drawback of PCL is that the transmitted waveform is not within the control of the radar designer. As a consequence, the target echoes may be masked by the disturbance contribution (i.e. direct signal and multipath): this can occur even in the presence of a large range-Doppler separation because of the high sidelobes level of the signal ambiguity function. To counteract these effects, proper processing techniques have been designed to enable effective target detection and localization [8]-[11]. However, these techniques have been mostly demonstrated in outdoor scenarios while few results are available for indoor localization and tracking.

Therefore, the first objective of this paper is to demonstrate the surveillance capability of WiFi-based PCL in indoor environment. To this purpose, the above techniques are tailored to face the specific challenges of the considered application and validated using real datasets. An experimental setup developed at the University of Rome "La Sapienza" is employed in order to perform different acquisitions against human targets. The reported results prove the actual possibility to detect and accurately track persons moving in realistic indoor environment and, in turn, demonstrate the effectiveness of the proposed signal processing techniques. We recall that a similar analysis was conducted by the authors in [10] and [14], against vehicular targets in outdoor scenarios, which clearly account for very different operative conditions. Therefore the results reported in this paper nicely complete the study of the practical effectiveness of the conceived sensor in solving real-world problems and extend the range of possible applications.

The second main goal of this paper is to provide the PCL sensor with the advanced capability to obtain high resolution cross-range profiles of moving targets. This could be an invaluable characteristic in indoor scenarios as it would yield an improved resolving capability to be exploited against the typically high concentration of targets moving in the surveyed scene. In fact we recall that WiFi transmissions allow a range resolution typically limited to tenths of meters, due to the limited frequency bandwidth occupied by the available signals (e.g. 11-18 m, depending on the adopted modulation). For these reasons, in [14] we investigated the possibility to exploit the motion of the target itself in order to achieve a high resolution in the cross-range direction (up to tens of centimeters) by applying Inverse Synthetic Aperture Radar (ISAR) processing techniques.

This is demonstrated in this paper with reference to an experimental test against human targets in indoor environment. The reported example clearly shows that, by extending the coherent processing interval up to a few seconds allows to effectively discriminate closely spaced targets moving in a hall, whereas they could not be resolved by a conventional processing.

In addition, we observe that the capability to obtain high resolution cross-range profiles of moving man-made objects would potentially enable the automatic classification of designated targets. This could be a valuable characteristic for many indoor surveillance applications such as in the field of automated guided vehicles in manufacturing lines, asset navigation and tracking or indoor unmanned vehicles navigation

Preliminary results along this line have been reported in [14] proving that the disturbance cancellation stage is a mandatory step not only for target detection but also for the ISAR profiling; nevertheless the background removal can have a non negligible effect on the target signal in input to the ISAR processing thus potentially degrading its cross-range profile formation.

This problem is even more severe in indoor scenarios where strong multipath contributions are expected to affect the received signals. As a consequence, the processing techniques described in [14] might yield limited performance especially when accurate profiling is required. Therefore in this paper, an alternative cancellation approach is introduced to obtain an effective removal of such disturbance while preserving the target contribution and, consequently, the quality of the ISAR processing. Based on an iterative target preserving algorithm, the proposed processing strategy is shown to overcome the limitations of the other cancellation approaches. The effectiveness of the proposed technique has been preliminary verified against data sets obtained by injecting synthetic target returns into the real background; then it has been tested against real vehicular targets moving in a parking area. The reported results prove that reliable cross-range profiles can be achieved, fruitfully exploitable by a classification scheme based on an appropriate signatures database.

The paper is organized as follows. In Section II the WiFi-based PCL processing scheme is briefly recalled. Section III shows the results obtained by applying the above scheme to several real data sets acquired against people walking in a hall: the results are quantified in terms of detection and localization capability of the human targets. Section IV summarizes the main steps of the ISAR processing for improved cross-range resolution (sub-section IV.A) and its potentialities are demonstrated with reference to human targets moving in indoor scenario. Section V introduces the innovative cancellation approach able to preserve the quality of the ISAR products (Section V.A) and its effectiveness is analyzed in section V.B against synthetic target echoes injected in real stationary

background. In addition, the performance of the conceived technique and the resulting cross-range profiling capability of the WiFi-based PCL sensor are verified in Section VI against real moving man-made targets. Finally, in Section VII we draw our conclusions.

II. WiFi-based PCL processing scheme

The basic WiFi-based PCL processing scheme for target detection designed by the authors has been fully described in [9]. Possible approaches to target localization have been investigated in [10] using different sets of measures whereas in [14] we define the required steps for obtaining a cross-range profile of the observed targets via the application of ISAR techniques.

The resulting overall processing scheme is depicted in Fig. 1. In this section we briefly summarize the blocks relevant to the target detection and localization tasks, paying special attention to the adjustments made to guarantee their effectiveness in the considered indoor application.

The signal reflected from the target is collected by the main PCL receiver (known as surveillance channel) while another receiver (known as reference channel) is adopted to collect the transmitted signal. In the considered scenarios, the PCL sensor is typically installed very close to the WiFi access point (AP) exploited as illuminator of opportunity; therefore, assuming the transmitter (TX) to be partially cooperative, its signal can be spilled from the TX antenna path using a directional coupler. If this is not the case, alternative approaches can be exploited to recover the transmitted signal, i.e. using a dedicated antenna or demodulating/re-modulating the signal received at the surveillance channel [9].

Since the transmitted waveform is not within the control of the radar designer, high sidelobes or undesired peaks appear in the corresponding Ambiguity Function (AF). Therefore the reference signal must undergo a modulation-dependent conditioning stage aimed at improving the resulting mismatched AF in the range dimension [16].

Then the reference signal is exploited to remove undesired contributions in the surveillance channel due to the direct signal from the TX and its multipath rays (i.e. bounces on stationary obstacles). To this purpose we resort to a modified version of the adaptive cancellation approach presented in [17], the Extensive Cancellation Algorithm (ECA), which operates by subtracting from the surveillance signal $s_{surv}(t)$ proper scaled and delayed replicas of the reference signal $s_{ref}(t)$. Specifically, by sampling the received signals at f_s and assuming that the multipath echoes are backscattered from the first K range bins, the output of the ECA is evaluated as:

$$s_{ECA}[n] = s_{surv}[n] - \sum_{k=0}^{K-1} \alpha_k s_{ref}[n-k] \qquad (1)$$

The filter coefficients $\boldsymbol{\alpha} = [\alpha_0 \ \alpha_1 \ \cdots \ \alpha_{K-1}]^T$ are evaluated by resorting to a Least Square (LS) approach that minimizes the power of the signal at the output of the filter:

$$\boldsymbol{\alpha} = (\mathbf{S}_{ref}^H \mathbf{S}_{ref})^{-1} \mathbf{S}_{ref}^H \mathbf{s}_{surv} \qquad (2)$$
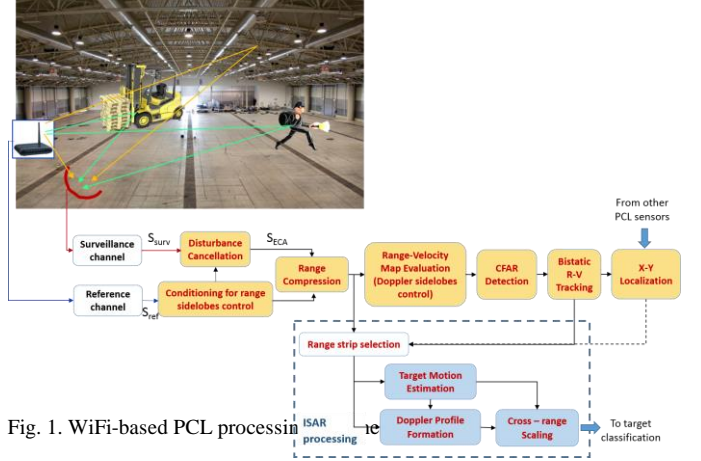

Fig. 1. WiFi-based PCL processing scheme

where $\mathbf{s}_{surv}$ is a $N \times 1$ vector containing N consecutive samples of the surveillance signal and $\mathbf{S}_{ref}$ is a $N \times K$ matrix whose columns are the delayed versions of the reference signal.

Notice that for the indoor application, the filter length K can be limited to few tenths of taps since the equivalent path length of the main multipath contributions is expected to not exceed few hundreds of meters. In addition, the vectors' length N in (2) has to be carefully selected as it determines the signal fragment (namely the batch duration) over which the filter weights are estimated so that it affects the capability to adapt to the varying characteristics of the environment [17]. However, reducing the batch duration widens the filter cancellation notch in the Doppler dimension, so that it should be traded with the minimum target detectable velocity to be guaranteed. The performed analysis allowed us to select batch durations between 80 and 120 ms for the indoor application; these values were verified to yield remarkable cancellation performance against the very slowly varying characteristics of the environment while enabling the detection of people moving in a building. The above constrains might be relaxed when operating with partially overlapped batches (i.e. by updating the filter coefficients after $N' < N$ samples); obviously this is paid in terms of computational load.

After the cancellation stage, target detection is sought by evaluating the bistatic Range-Velocity map over short coherent processing intervals (CPI). CPI durations between 0.1 s and 0.5 s have been verified to be a reasonable compromise between achievable SNR gain and expected range/velocity walk of typical indoor targets. Specifically, due to the pulsed nature of the WiFi transmissions, the range compression is obtained by cross-correlating the surveillance and the reference signals on a pulse basis. Then, the velocity dimension is synthesized by applying a Fast Fourier Transform (FFT) over the pulses available in the CPI.

Notice that possible limitations to the WiFi-based PCL operation at this stage might be due to interference from other APs used in the same area. However, if the interfering AP operates on adjacent (partially overlapped) frequency channels, its transmission is expected to yield just a limited increase in

the system noise floor. This can be explained by observing that (i) the received interfering signal does not correlate with the reference signal adopted for matched filtering, and (ii) the probability of collision between the same pair of APs is usually low so that only a small percentage of pulses in the CPI are affected by such interfering transmission. Different considerations apply when the interfering AP is operated in the same WLAN channel used by the AP of opportunity. In this case, the occurrences of collisions are substantially avoided thanks to the implementation of carrier sense multiple access (CSMA) protocols. Therefore, the effect of an interfering AP would be to inhibit a high rate transmission of pulses by the AP of opportunity. From a radar application point of view, this might upper limit the equivalent pulse repetition frequency and yields a highly variable temporal separation among consecutive pulses. In typical situations, this effect is responsible of high sidelobes to appear in the AF of the WiFi signal along the Doppler dimension. However, in [18] we have shown that it is possible to design effective taper functions to control such sidelobes at least in the Doppler range of interest.

A constant false alarm rate (CFAR) threshold is then applied on the obtained map to automatically detect the potential targets thus providing a first target localization over the bistatic range/velocity plane. The measures collected at consecutive observations can be used to perform a line tracking over this plane. Using a conventional Kalman algorithm allows to reduce the false alarm rate while yielding more accurate range/velocity estimations.

By combining the measures available at multiple PCL sensors, the target 2D localization in local Cartesian coordinates can be obtained [10]. In particular a couple of closely spaced surveillance antennas allows the estimation of the Direction of Arrival (DoA) of the detected target echo by applying an interferometric approach. In addition, multilateration techniques can be employed to localize the target based on the bistatic range measurements performed at properly dislocated PCL sensors.

The results obtained with the above processing scheme have been reported in different contributions showing its effectiveness mostly in outdoor scenarios, [8]-[10]. In the next Section, the potentialities of the proposed WiFi-based PCL sensor are investigated with reference to indoor applications.

III. INDOOR TARGET DETECTION AND LOCALIZATION: EXPERIMENTAL RESULTS

In the last years, the authors have been involved in two EU Projects aimed at the demonstration of the effectiveness of WiFi-based PCL sensors for the surveillance of airport terminal areas [12]-[13]. In this context, extensive test campaigns have been carried on for different indoor scenarios using cooperative human targets.

The passive radar prototype developed at the DIET Department of the University of Rome "La Sapienza" has been employed [19]. It consists of four receiving channels providing a fully coherent base-band down-conversion of the input signals; these are then synchronously sampled at 22 MHz and stored for off-line processing.
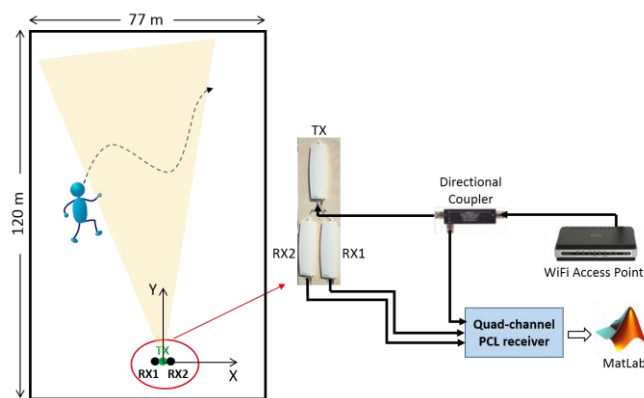

Fig. 2. Sketch of the experimental setup.

In this paper we report the results obtained against the data collected with the experimental setup depicted in Fig. 2. The PCL receiver has been fielded in a wide exhibition hall of the "Nuova Fiera di Roma" whose size is comparable with an airport's terminal (see picture on the upper left corner of Fig. 1). In particular, the exhibition hall is approximately 77 meters wide and 120 meters long. An (X,Y) coordinate system has been defined with the X axis aligned with the short side of the hall and the Y axis oriented toward its center, being the origin of the system located on the TX antenna.

A commercial WiFi AP was used as transmitter of opportunity. Its output was connected to the transmitting antenna while a directional coupler was used to send a -20 dB copy of the transmitted signal (the reference signal) to the first receiving channel of the quad-channel PCL receiver. Two surveillance antennas (RX 1 and RX 2) were employed, aligned along the X direction at a distance of 12 cm which gives a 45° ambiguity for the target DoA estimation. The transmitting antenna was mounted at a height of about 2 meters from ground while the two receiving antennas were placed about 40 cm below, in a quasi-monostatic configuration, and steered toward the positive Y axis. All the antennas are commercial WiFi panel antennas and are characterized by a gain of 12 dBi, a front-to-back ratio of 15 dB and beamwidths equal to about 80° and 23° on the horizontal and the vertical plane, respectively.

The router was configured to transmit in channel 1 of the WiFi band (2412 MHz). It was set up to roam for connected devices emitting a regular Beacon signal exploiting a DSSS modulation at 3 ms intervals.

About 60 different tests have been performed using one or two human targets walking simultaneously in the area to be surveyed. In the following, for illustrative purposes, we will report the results of the three tests described below:

- test T1 [Fig. 3(a)]: a man moves toward the transmitter of opportunity with roughly constant velocity along the Y axis (i.e. DoA equal to zero degrees);

- test T2 [Fig. 3(b)]: two men walk along crossing paths. In particular, they initially move closer together; once they have come across, they contemporaneously change they
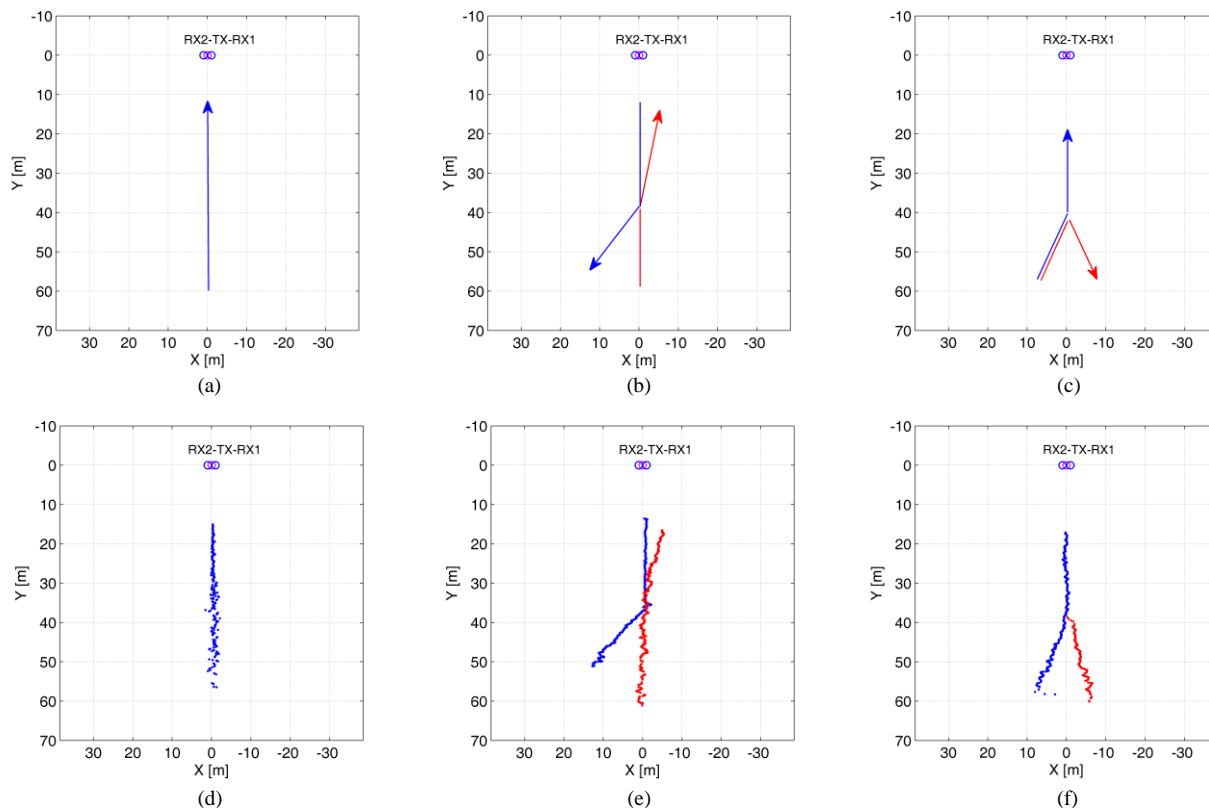
Fig. 3. Real target trajectories for (a) Test T1; (b) Test T2; and (c) Test T3. PCL localization results for (d) Test T1; (e) Test T2; and (f) Test T3.

walking directions departing from the Y axis with different angles;

- test T3 [Fig. 3(c)]: two men move along partially overlapping paths. In particular, they initially walk on the same direction with a constant separation of about 1 m; then they abruptly change their heading, going towards opposite sides of the hall.

The data collected for each test covers a length of time equal to 25 sec and has been processed according to the WiFi-based passive radar processing scheme of Fig. 1. In particular, the ECA is applied with a batch duration equal to 100 ms over a range of 300 m; a coherent integration time of 0.5 s is used to evaluate the bistatic range-velocity map over consecutive portions of the acquired signals (frames) with a fixed displacement of 0.1 s (10 frames per second are thus obtained); and target detection is performed by resorting to a standard cell-average CFAR threshold with a probability of false alarm equal to 10^{-4}.

As an example, in Fig. 4(a) we report, on the same range/velocity plane, the raw detections collected along the whole acquisition (25 seconds) for test T1 (black '×' markers). As is apparent different kinds of detections can occur that might be classified as follows:

(i) Detections which are likely to correspond to the target returns as they are compliant with the test geometry. It is worth noticing that such detections spread over the velocity dimension; this can be reasonably related to the motion of the legs and arms of the human body that induce

Doppler modulations around the main target Doppler shift (micro-Doppler effect).

(ii) Detections resulting from the multipath effect caused by reflections of the target echo over either the walls or the ceiling of the hall; in fact they draw a range/velocity trajectory that can be predicted based on the real target trajectory by applying geometrical optics rules.

(iii) Spurious Doppler peaks due to the PCL receiver non-idealities. These are responsible for detections appearing for all the performed tests at constant velocity and very short ranges.

(iv) False alarms due thermal noise and disturbance residuals; in this specific case, few false alarms arise thanks to the '2-out-of-2' criterion adopted to integrate the detection results separately obtained at the two surveillance channels. Anyway isolated false alarms might be easily discarded by a tracking algorithm.

The output of a conventional Kalman tracking algorithm operating over the range-velocity plane is also reported in Fig. 4(a) (red circles). The plot association stage exploits a nearest neighbour approach that follows a careful selection of the raw detections. In fact, while the analysis of the complex target micro-Doppler signature might be useful if target recognition is required, for the purpose of our analysis, the raw detections arising from this effect are properly discarded by retaining a single detection for each range cell where the CFAR threshold has been exceeded.

The phase difference between the range/velocity maps

obtained for RX 1 and RX 2, taken at the target detection point, is then exploited to obtain the target DoA estimation. The estimated target DoA along the performed acquisition is shown in Fig. 4(b) for the longest track identified on the range/velocity plane in Fig. 4(a). As is apparent, the reported result is well in line with the test T1 geometry as the target moves along the Y axis.

Finally, by jointly exploiting bistatic range and DoA measurements, target 2D localization is obtained using the approach described in [10]. The result obtained for the target of test T1 is reported in Fig. 3(d). Correspondingly, Fig. 3(e)-(f) report the X-Y output for tests T2 and T3, respectively.

As is apparent, in all cases, only small deviations are observed with respect to the real targets trajectory [see Fig. 3(a)-(c)]; these are mainly due to the target range/DoA estimation accuracies and their projection on the X-Y plane. Anyway, better results are expected by exploiting multiple PCL sensors properly dislocated around the hall [10]; moreover the achievable positioning accuracy can be increased by applying a second tracking stage on the Cartesian plane.

With reference to the experimental tests involving two targets (i.e. T2 and T3), we observe that the conceived system is able to correctly identify and track the two men moving in the hall as far as they can be distinguished in the range/velocity plane; in particular, when the targets move towards opposite directions they yield echoes with opposite Doppler frequencies.

In contrast, in test T3, only a single target is recognized and tracked in the first part of the acquisition as the two men walk close each other.

Obviously this is a consequence of the limited resolution provided by the WiFi-based PCL, especially in the range dimension. Therefore, whereas the above results clearly show the promising characteristics of the conceived sensor for indoor target localization and tracking in surveillance applications, it is of great interest the study of alternative processing techniques able to provide an improved resolution capability on the observed targets, along the line investigated in [14].

IV. ISAR TECHNIQUES FOR IMPROVED CROSS-RANGE RESOLUTION

A. Resolution improvement via ISAR techniques

As is well known, the WiFi-based passive radar guarantees equivalent monostatic range resolution of 11 m or 18 m by exploiting the bandwidth of DSSS or OFDM transmissions, respectively [7]. Additional resolution in cross-range direction could be achieved by coherently processing the returns from the target of interest when observed at different aspect angles. Particularly in ISAR the angular aperture needed to this purpose is obtained by exploiting the motion of the target itself, [15]. Therefore in [14] we have shown that a cross-range resolution considerably higher than the range resolution can be achieved by applying ISAR techniques to targets with a motion component in the cross-range direction.

The main required processing steps are sketched in Fig. 1 in the dashed frame. Once a moving target has been detected, the corresponding range strip is selected from the compressed data
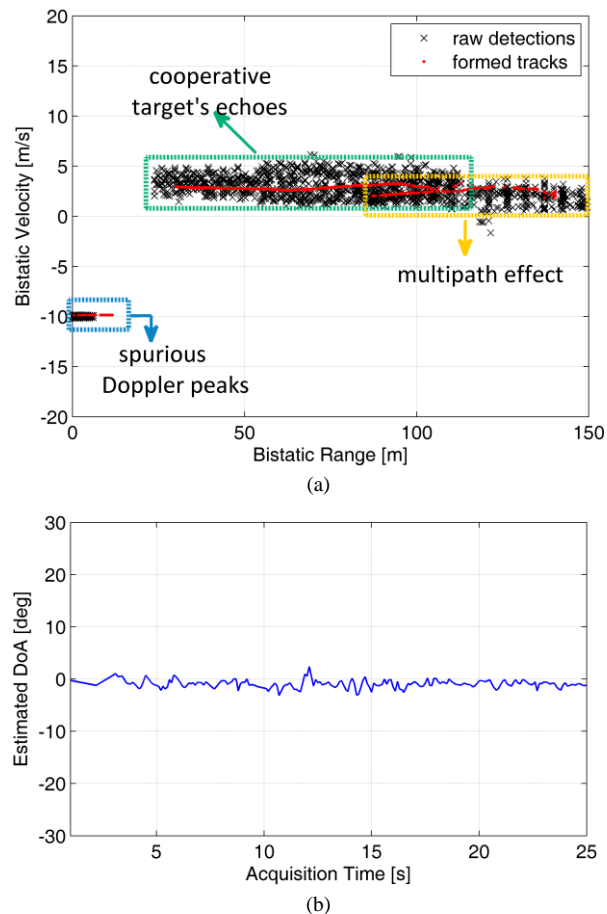

Fig. 4. Target detection and DoA estimation results for test T1. (a) Plots and tracks over the range/velocity plane. (b) Estimated target DoA vs time.

by retaining the range bins of interest and fed in input to the ISAR processing block constituted by the cascade of target motion estimation, cross-range profile focusing and scaling. The target phase history in the ISAR CPI is approximated by a M degree polynomial law with coefficients a_i $(i = 1,..,M)$. Consequently the target motion is estimated by searching for the set of coefficients $\hat{a}_i$ that better compensates the migration through both range and Doppler resolution cells and thus provides the best quality of the focused profile according to a specific cost function. Once the target motion parameters are available, the cross-range profile is formed and properly scaled by mapping Doppler frequencies into cross-range distances.

In [14] further details are reported on the search strategy, on the objective function adopted for the autofocus, and on the focusing/scaling stage. Here it is worth mentioning that, for the considered geometries, the degree of the polynomial is typically selected to be $M \geq 3$ because long coherent processing intervals (order of several seconds) are required to obtain remarkable resolutions. However, we point out that the estimation procedure can be fruitfully initialized by the rough motion estimation provided by the PCL tracking stage.

The proposed ISAR mode has been tested in [14] against real data sets for both monostatic and bistatic geometries. The reported results showed that: (i) the disturbance cancellation stage is essential for target detection and motion estimation, (ii)

the disturbance cancellation has a non negligible effect on the target signal fed in input to the ISAR processing so that it might reduce the quality of the ISAR products. In fact, the ECA strongly attenuates the target signal components at low Doppler frequencies since they are recognized as stationary contributions and included in the adaptive estimation of the cancellation weights. As a consequence, a considerable part of the target Doppler chirp can be lost and this potentially cause a degradation of the ISAR products. This degradation can occur in the case of slow-moving targets as well as in the case of targets moving along the cross-range direction, that are the most interesting ones to apply the ISAR processing schemes.

Obviously different applications impose different constraints and requirements on the quality of the ISAR products so that this potential degradation might be appreciable or not. Particularly when considering human targets the strong requirement is on the resolution capability enabling the separation of the different targets. In contrast, when dealing with man-made targets (such as vehicles), the requirement is on the accurate separation and extraction of the different scattering centres of the same target so that ATR (Automatic Target Recognition) procedures could be enabled. While standard quality ISAR products can allow the separation of different targets, enhanced quality products are essential for classification purposes. Therefore in the remaining part of this section we focus our attention on the case of human targets and the processing scheme in Fig. 1 is applied; then the case of man-made targets is considered in the following sections where an enhanced ISAR profiling technique is proposed (section V) and the results achievable via its application are presented (section VI).

B. Experimental results against human targets

Potential of ISAR techniques in resolving closely spaced human targets moving in a cluttered indoor scenario is here demonstrated by using live data acquired by means of the PCL receiver described in section III. The PCL receiver has been fielded in the canteen of the School of Engineering at University of Rome "La Sapienza" whose size is approximately equal 11 meters wide and 28 meters long (Fig. 5). An (X,Y) reference system has been defined similarly to that in Fig. 2. Tests have been performed using two human targets about 2 meters apart moving in cross-range direction (i.e. trajectory parallel to X axis) with approximate speed 1.3 m/s, distance of minimum approach R_0=24.4 m and overall test duration equal 10 sec.

The acquired data has been processed via the whole processing scheme in Fig. 1 with ECA applied with a batch duration set to 400 ms over a range of 300 m and the bistatic range-velocity map evaluated over a CPI of 0.5 s. A cut of the bistatic range-Doppler map at the range bin interested by the two human targets is reported in Fig. 6 (blue dashed curve). We can observe that the two targets give rise to the presence of a single strong peak meaning that the two targets can be detected but not resolved. By increasing the coherent processing interval (3 sec) and feeding the ISAR processing block (with M=3) the red curve in Fig. 6 is obtained. We observe that the increased
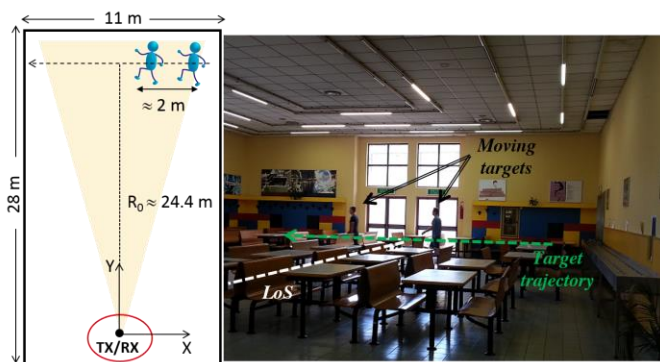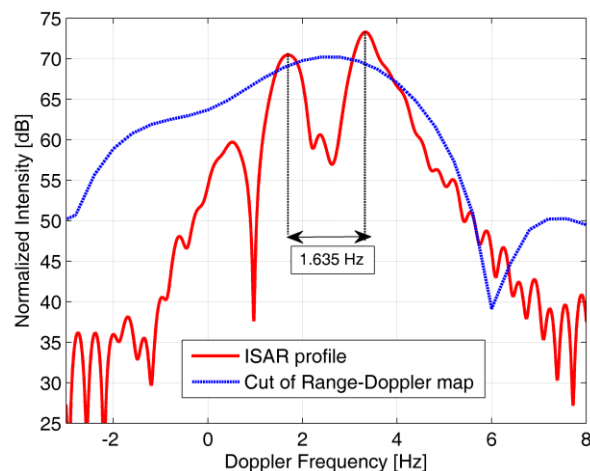

Fig. 5. Sketch of acquisition geometry.

Fig. 6. Cut of the Range-Doppler map (CPI=0.5 sec) and ISAR profile (CPI=3 sec) comparison.

CPI provides an improvement in terms of both Doppler resolution and target peak power. Particularly, the two targets give rise to the presence of two clearly resolved peaks whose Doppler separation (1.635 Hz) scaled accordingly to the estimated cross-range speed (1.3130 m/s) provides 1.865 meters which is largely in agreement with the actual separation between the targets.

The reported results clearly show that the motion of the targets can be fruitfully exploited to improve cross-range resolution so that closely spaced targets can be effectively discriminated whereas they could not be resolved by a conventional processing. Moreover the characteristics of the considered indoor scenario demonstrates the potential of the proposed approach in cases of practical interest.

V. ENHANCED ISAR PROFILING TECHNIQUE

When dealing with man-made targets typically ISAR techniques are employed to achieve high resolution products to be exploited by the classification and recognition procedures. In this case high quality products are needed in order to assure a reliable classification. As mentioned before ISAR techniques applied in cascade with conventional ECA can result in a quality degradation of the ISAR products. Therefore, in [14], an alternative cancellation approach has been presented. According to this approach, the cancellation filter weights have to be estimated and updated only at signal fragments that do not

contain target contributions at low Doppler frequencies (being this information made available by the previous tracking stage). This in principle allows to remove the strongest disturbance components in the observed scene as they are stationary during the ISAR CPI. In contrast this prevents the cancellation of the target echoes as it crosses the zero-Doppler along its motion.

Unfortunately, this approach has some limitations that may make it ineffective in the considered application. In particular, in indoor scenarios, due to the possibly high density of targets, it could be very unlikely to identify a signal fragment that does not include low Doppler target echoes. As a result, the filter weights would be seldom updated so that the cancellation capability of slowly varying disturbance contributions can be seriously degraded. Notice that the slowly varying characteristics of the stationary background can be also ascribed to the instability of the employed receiver (phase noise of local oscillators, time jitter of ADC, etc.) so that the possibility to frequently update the filter coefficients is critical.

For the reasons above, in this paper we present an innovative target preserving disturbance cancellation technique able to overcome the limitations of previous approaches and to provide enhanced quality profiles of moving man-made targets. Particularly sub-section V.A describes the new technique while sub-section V.B analyses the corresponding Point Spread Function (PSF) by injecting a moving point-like object into the real background.

A. Iterative target preserving cancellation algorithm

To preserve the target signal for the following ISAR processing, its contribution to the received signal should be properly reduced prior to estimating the cancellation filter coefficients. To this purpose, the proposed approach exploits the output of the ISAR profiling stage to retrieve from it the signal contribution concerning the considered target and uses this recovered component to clean the received surveillance signal. In this way the estimation of the cancellation filter weights can be repeated using a signal with "target reduced" characteristics. By iteratively repeating the above steps, progressively a "target free" signal is made available for filter weights estimation and the low-frequency components of the target returns are better reconstructed.

Thus the proposed technique somehow follows a CLEAN-like philosophy [21]. The CLEAN algorithm has been used in passive radar in [20] and [11] with the purpose of removing stationary clutter and direct signal contributions from the received signal by operating in the signal domain or in the range–Doppler space. In contrast a multistage algorithm for strong target removal has been presented in [17] where the contributions of previously detected target are removed from the received signal on short CPIs (namely, those exploited for target detection).

In this paper, the target cancellation stage benefits of an increased CPI duration that allows a more accurate estimate of the target contribution to be removed. In this regard, the proposed strategy resembles the approach of CLEAN techniques adopted in conventional radar imaging, [21], aimed at extracting those scatterers of the imaged targets typically masked by the sidelobes of dominant ones. This task is achieved by estimating the contribution from the dominant scatterers and progressively cleaning the image from them so that weak
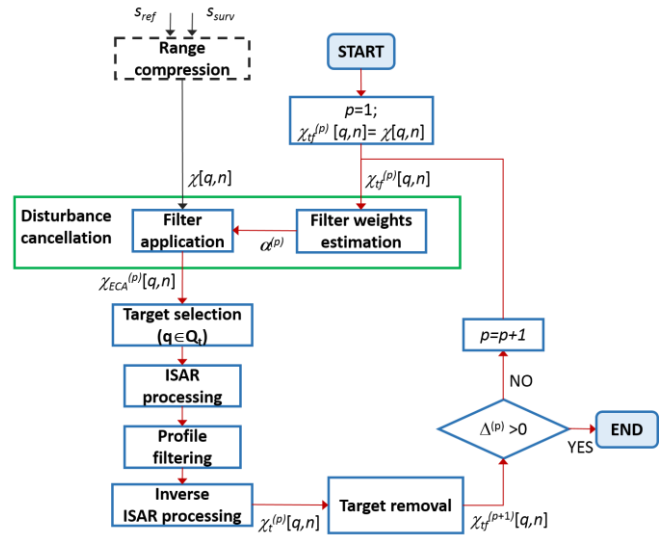

Fig. 7. Block diagram of the iterative target preserving ISAR profiling technique.

scatterers could be observed. In contrast, the objective of the proposed approach is to feed the adaptive stage of the ECA with a "target free" version of the received signal.

The block diagram of the proposed iterative target preserving (ITP) technique is sketched in Fig. 7.

First of all we observe that the disturbance cancellation has to be repeated at each iteration of the proposed algorithm. According to the processing scheme presented in Fig. 1, this stage precedes the range compression so that an iterative cancellation approach would require a high computational load.

However, we point out that the two stages above can be nicely swapped by observing that

i. the cancellation filter can be applied against the range compressed data $\chi[q, n]$, (where q is the range bin index and n accounts for the slow-time), and

ii. the estimation of the filter weights might follow the evaluation of both the reference signal autocorrelation and the cross-correlation between the reference signal and the surveillance signal. In fact, the matrix $\mathbf{S}_{ref}^{H}\mathbf{S}_{ref}$ ($K \times K$) in (2) represents an estimated version of the reference signal autocorrelation matrix accounting for the first K time bins and obtained by averaging over the selected batch duration. Similarly, the K-dimensional vector $\mathbf{S}_{ref}^{H}\mathbf{s}_{surv}$ in (2) represents an estimate of the cross-correlation between the reference signal and the surveillance signal which can be evaluated by averaging the results of the range compression stage over consecutive pulses. With the above position, the proposed approach can be easily integrated, as an advanced mode, in the basic processing scheme devoted to target detection and tracking.

At the p-th iteration of the proposed algorithm the following steps must be performed:

1) The weights $\boldsymbol{\alpha}^{(p)}$ of the ECA are adaptively estimated based on the current "target free" version of the surveillance signal $\chi_{tf}^{(p)}[q, n]$ after range compression. At

the first iteration ($p=1$) this signal coincides with the original range compressed signal.

2) The filter weights $\boldsymbol{\alpha}^{(p)}$ are applied against the original surveillance signal to obtain its disturbance free version $\chi_{ECA}^{(p)}[q,n]$. It has to be noticed that, at the first iteration, this output coincides with the standard ECA applied against the original data.

3) The signal at the selected target range strip is extracted (i.e. $\chi_{ECA}^{(p)}[\bar{q},n] \mid \bar{q} \in Q_t$, where Q_t identifies the range bins spanned by the target along its motion) and fed in input to the ISAR processing stages that include the target motion estimation and its cross-range profile formation in the Doppler dimension. Range strip selection is enabled by the information provided by the tracking output.

4) The target profile is properly filtered to reject the residual background and to enhance the selected target contribution; to this purpose a rectangular window is adaptively defined, based on the selection of a proper threshold to be applied against the current cross-range profile to identify its essential portions.

5) Then a reverse focusing is applied to the filtered ISAR profile to recover the current estimate of the target signal in the range-compressed slow-time domain $(\chi_t^{(p)}[\bar{q},n] \mid \bar{q} \in Q_t)$. Specifically this stage includes:

- an inverse Fourier transform to move from Doppler frequency to slow time domain;
- the insertion of the range migration that can be achieved by (i) transforming the data in the fast-frequency slow-time domain, (ii) applying a linear phase term depending on $\hat{a}_1$ (estimated target Doppler centroid), and (iii) inverse Fourier transforming the data back in the range – slow time domain;
- the insertion of the Doppler migration resulting from the estimated target motion parameters (i.e. $\hat{a}_i$, $i > 1$).

6) Finally, the recovered signal is subtracted from the original surveillance signal to provide the new "target free" version to be exploited at the following iteration:

$$\chi_{tf}^{(p+1)}[q,n] = \begin{cases} \chi[q,n] - \chi_t^{(p)}[q,n] & q \in Q_t \\ \chi[q,n] & q \notin Q_t \end{cases} \quad (3)$$

Notice that, as the target return is better recovered, its contribution to the ECA weights estimation is progressively limited thus reducing its "auto-cancellation" effect. In contrast, the target-free signal can be successfully exploited to estimate the stationary disturbance characteristics so that its removal is kept guaranteed, or even improved, as the algorithm progresses.

The algorithm should be arrested at the time that the signal $\chi_{tf}^{(p)}[q,n]$ is likely to contain only stationary scatterers contributions (or possibly contributions from other targets). To this aim, a simple stop condition can be defined based on the estimated power level of the target-free signal at the range bins of interest along the whole ISAR CPI:

$$P_{tf}^{(p)} = \sum_{q \in Q_t} \sum_n \left| \chi_{tf}^{(p+1)}[q,n] \right|^2 \quad (4)$$

This power level is expected to rapidly decrease at the first iterations where the target main components are easily recovered and subtracted from the available signal, while the reduction of $P_{tf}^{(p)}$ might become slower as p grows. Therefore, to limit the required computational load, the algorithm can be stopped when this parameter reaches a desired value (depending on the estimated noise floor) or when its slope is sufficiently flat. However, we have experimentally verified that this parameter usually exhibits a minimum as a function of the iteration number (this will be shown in the next section). Consequently, a reasonable stop condition can be based on the following rule:

$$\Delta^{(p)} = P_{tf}^{(p+1)} - P_{tf}^{(p)} > 0 \quad (5)$$

When such condition holds, the output target Doppler profile is assigned to the last ISAR stage output and, as the final step, undergoes cross-range scaling.

Obviously the enhanced quality of the achieved ISAR profile is paid in terms of an increased computational cost of the iterative technique with respect to the standard one (basically almost coinciding with the first iteration). If we indicate with P the generic number of iterations needed before reaching the stop condition then the overall computational cost of the iterative technique in principle increases linearly with P. However it is worth observing that:

- as demonstrated by the results shown in the following, typically few iterations (P in the order of 10÷20) are needed to reach the stop condition;
- at the p-th iteration, with p≥2, results from the previous iteration can be suitably exploited in order to limit the selected range strip to the strictly needed range bins (thus limiting the data to be processed) and to initialize the motion estimation techniques (thus requiring not a completely new estimate but a refinement of the previous step).

Based on the two above considerations we can conclude that the increase of the computational cost required by the iterative technique is still manageable and therefore the proposed approach is suitable for application to solve real-world problems.

B. Results against synthetic target echoes injected in real stationary background

Aiming at understanding the effect of the cancellation techniques on the ISAR PSF of the system, some controlled tests have been performed. To this purpose an acquisition of duration 6 seconds is considered in the following that contains only the returns from the stationary scene (namely, no targets where employed in this test). The echoes of a fictitious point-like target has been then injected in the collected data.

In particular it is assumed that, during the ISAR CPI of 6 s, the target moves from point $(x_A, y_A) = (-13.5m, 50m)$ to point $(x_B, y_B) = (13.5m, 50m)$ with constant velocity $v_x = 4.5$ m/s,

distance of minimum approach $R_0 = 50$ m and signal-to-noise ratio SNR = -20 dB.

Fig. 8(a) shows the Doppler spectrum of the overall signal containing both target and clutter contributions (black curve) compared to the theoretical Doppler spectrum of the target only signal (red curve) which is used as benchmark. The signals are scaled so that the 0 dB level represents the system noise floor. As is apparent a strong component appears at zero Doppler due to the stationary scene; this is well above the contribution of the fictitious scatterer which yields a rectangular shaped spectrum spanning about 40 Hz around 0 Hz.

In [14] the strong stationary contribution has been shown to prevent an effective target motion estimation so that the disturbance cancellation stage can be regarded as a necessary step for the successful formation of target cross-range profiles.

Therefore, in Fig. 8(b) we report the result obtained after a standard cancellation based on the ECA (green curve). As is apparent, the disturbance component is effectively removed. However, as expected, the cancellation filter has dramatically distorted the target spectrum shape at low Doppler frequencies by inserting a cancellation notch. This clearly shows the "auto-cancellation" effect of the target echoes; basically these echoes strongly affect the cancellation filter evaluation as long as the target moves with low radial velocity with respect to the TX/RX so that they are indiscriminately removed together with the stationary scene. Such effect certainly degrades the effectiveness of the subsequent ISAR processing which needs the entire Doppler frequency history of the target to generate the clairvoyant cross-range profile. Specifically, this yields a corresponding SNR loss that in turn results in a reduced accuracy in the target motion estimation and in a corresponding loss in terms of cross-profile amplitude. Moreover, depending on the portion of the target spectrum that has been cancelled (i.e. central or side part), the above effect might cause severe ambiguities or cross-range resolution degradation.

In the considered case-study, the observed warp of the target spectrum mainly yields an increased sidelobe level in the achievable cross-range profile. This is shown in Fig. 9 that reports the cross-range profile obtained for the fictitious target after the application of the conventional ECA (green curve) compared to the clairvoyant, target only, profile (red curve) which represents the ideal ISAR PSF of the system. Correspondingly, Table I reports the main characteristics of the obtained cross-range profiles in terms of amplitude loss, cross-range resolution, and peak-to-sidelobe ratio (PSLR). The cancellation filter operates over partially overlapped batches of 0.1 seconds each, and the filter length K is set equal to 92, which corresponds to a bistatic range extent of about 500 m at the considered sampling rate. The reported profiles have been obtained by setting $M=3$.

As is apparent, the achievable PSLR is 4.17 dB when a conventional ECA approach is adopted for disturbance cancellation; this value has to be compared to the theoretical 12 dB obtained in the target-only case (notice that, by limiting the polynomial approximation of the phase history to the third order, uncompensated phase terms of higher orders are accepted that are responsible for a slight PSLR degradation with respect to the 13.26 dB expected for a point-like scatterer in the ideal case). Moreover, a significant amplitude loss is observed since much of the target spectrum has been cancelled by the ECA.
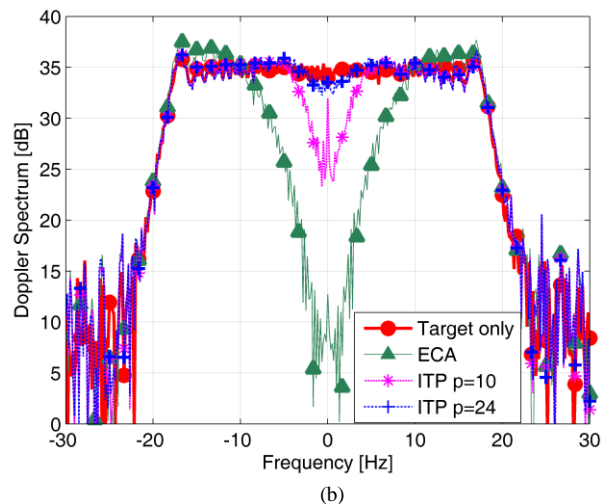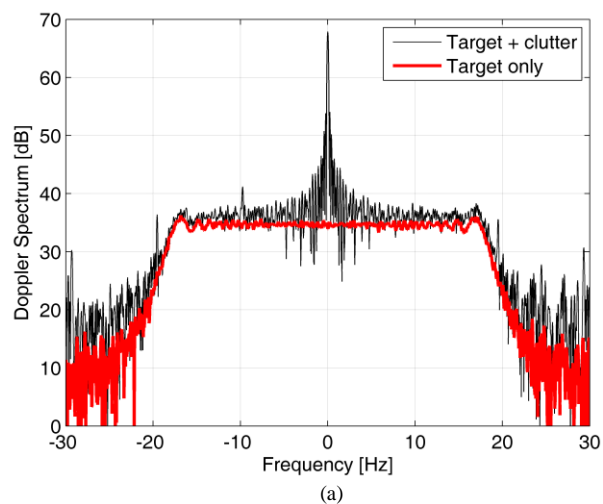

(a)

(b)

Fig. 8. Signal Doppler spectrum. (a) Before disturbance cancellation. (b) After disturbance cancellation using different techniques.
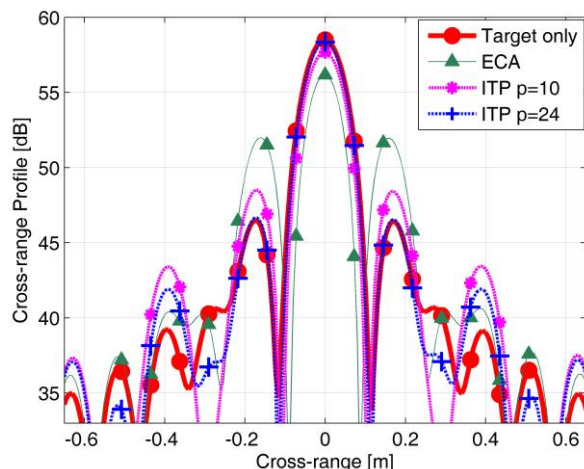

Fig. 9. Cross-range profiles for the fictitious target.

Finally, it is to be noticed that the slight increase in terms of cross-range resolution is just a misleading effect of the profile warp.

The results obtained after the application of the ITP technique are shown in Fig. 8(b) and Fig. 9 for an increasing number p of iterations (we recall that the conventional ECA coincides with

the first iteration of the proposed technique). As is apparent, as p increases, the target "auto-cancellation" effect is progressively smoothed so that the Doppler spectrum is comparable with the theoretical one [see Fig. 8(b)]. Correspondingly, the obtained cross-range profile resembles the clairvoyant target-only profile with only small deviations in the low side-lobes region (see Fig. 9). This depends on the threshold adopted in the ITP approach to identify the target contribution (in this case 20 dB below the highest target peak) which sets the dynamic range for the recovery of the target signal.

To investigate the reliability of the proposed stop condition, in Fig. 10 we show the residual power level $P_{tf}^{(p)}$ defined in (4) as a function of the iteration number p.

As is apparent, the main target contributions are rapidly gathered at the first iterations; however at least 20 iterations are required for the target signal to be better reconstructed. Notice that, as previously mentioned, the reported curve shows a minimum at p=24. Therefore, the algorithm can be arrested after p=24 iterations since this stage yields the best reconstruction of the target signal. This is also confirmed by the results obtained in terms of cross-range profile and its characteristics (see Table I). In particular, after p=24 iterations, the amplitude loss and the PSLR degradation have been almost totally recovered and the obtained cross-range profile concides with the theoretical one in the region encompassing the main lobe and first sidelobes.

VI. EXPERIMENTAL RESULTS AGAINST MOVING MAN-MADE TARGETS

In this section, the performance of the proposed strategy is analyzed against live data and compared to the conventional ECA. The considered data set has been collected by means of the same PCL receiver described in section III. However, aiming at understanding the potentialities of the conceived sensor also for applications of vehicles monitoring and classification, we have been compelled to perform the dedicated test campaigns in outdoor scenarios.

Specifically, the tests were performed in a parking area in front of a private building (see Fig. 11). A single surveillance antenna has been employed, mounted just below the transmitting antenna in a quasi-monostatic configuration. Again, an (X,Y) coordinate system is defined with the origin in the TX/RX antennas location.

Cars have been used as cooperative targets to demonstrate the practical effectiveness of the proposed approach. Two different tests (M1 and M2) were performed using one or two identical cars (i.e. Fiat Punto Evo) with length of about 4 meters. In both cases the vehicular targets move along the axis y=y₀=50 m (red dashed line in Fig. 11) at about v_x=4.5 m/s. Specifically, in test M1, a single car was present approximately crossing the point (x₀;y₀)≡ (0 m; 50 m) at the middle of the acquisition. For test M2 a second identical car was employed moving behind the first car with a separation of about 2-3 meters along the x-axis so that, at the middle of the acquisition, they were almost symmetrically displaced about the point (0 m; 50 m). The overall duration of each acquisition is 10 seconds;

TABLE I
CHARACTERISTICS OF THE CROSS-RANGE PROFILES OBTAINED FOR THE FICTITIOUS TARGET

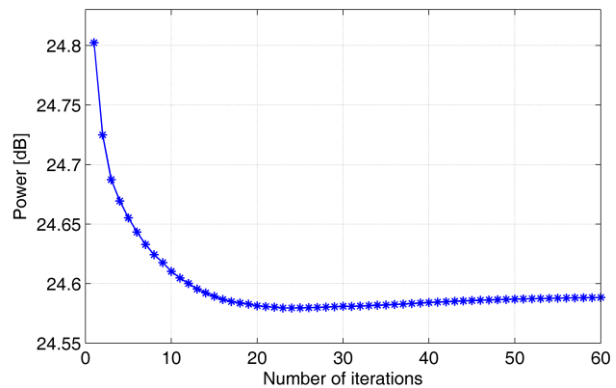|	Target only	ITP-based ISAR technique				
		Iter p=1 Conventional ECA	Iter p=5	Iter p=10	Iter p=20	Iter p=24
Amplitude Loss	0 dB	2.33 dB	1.35 dB	0.82 dB	0.27 dB	0.14 dB
Cross-Range Resolution	11.6 cm	10 cm	11.6 cm	11.6 cm	11.6 cm	11.6 cm
PSLR	12 dB	4.17 dB	7.62 dB	9.17 dB	11.13 dB	11.66 dB

Fig. 10. Estimated power level of the target-free signal at the range bin of interest as a function of the iteration number.
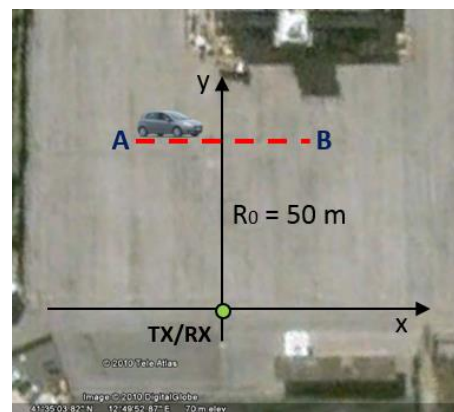

Fig. 11. Sketch of the acquisition geometry.

the results shown in the following have been obtained by using an ISAR CPI set to 6 s properly selected from the whole recording.

Fig. 12(a) compares the Doppler spectra obtained for test M1 in absence of the cancellation stage (black curve), using the conventional ECA (green curve), and after the iterative target preserving cancellation approach (blue curve). The latter algorithm has been arrested after 8 iterations according to the proposed stop condition since the power level $P_{tf}^{(p)}$ defined in (4) exhibits a minimum in p=8 [see Fig. 12(b)]. Moreover, in this case, the threshold adopted to identify the target contributions based on the current profile has been set experimentally at 13 dB.

As observable from Fig. 12(a) the original Doppler spectrum

is the sum of the targets contributions and a strong stationary contribution around the zero Doppler.

After the application of ECA, the disturbance component has been effectively removed but the filter cancellation notch in Doppler dimension has also reduced the target contribution at low frequencies. In contrast, the benefits of the proposed iterative algorithm are clearly visible as it better preserves the target spectral components at low Doppler frequencies while still guaranteeing an effective cancellation of the echoes from the stationary scene. This behavior resembles that shown for the fictitious target in section V.B: obviously in this case a less regularly shaped Doppler spectrum is observed because we are now dealing with a real target instead of the ideal point-like isotropic scatterer.

The corresponding cross-range profiles are shown in Fig. 13(a). We observe that, as for the case of the fictitious target, the newly proposed target preserving strategy yields an improvement of few dBs in terms of profile amplitude. In fact, the capability to preserve a greater portion of the target spectrum has been shown to improve the performance of the subsequent ISAR processing in terms of both target motion estimation and target focusing. This in turn should lead to the formation of more stable profiles to be exploited for the extraction of reliable information on the observed targets. To further demonstrate the reliability of the achieved results, Fig. 13(b) shows the cross-range profiles achieved for experiment M2. In this case the ITP algorithm stops after 16 iterations according to the stop condition in (4). As it is apparent, with both the ECA and the ITP cancellation approach, the profiles reveal the presence of two similar patterns characterized by three main peaks (labeled with capital letters) which correspond to the main scattering centers of the two identical cars used for the considered experiment.

As an example, in Table II we evaluate the distances between homologous points of the cars (i.e. profile peaks) from the cross-range profiles obtained with the ECA and the ITP approaches, respectively. Even if the actual value of this distance is not available, it is expected to be constant independently of the considered pair of peaks. Apparently, the values obtained for the three pairs of peaks are well in line with the test geometry (we recall that the length of each car is 4 meter and their separation along the path is about 2-3 m); however, for all the three considered pairs, the use of the iterative technique provides less scattered values, when compared to ECA, thus proving a more accurate extraction of the target scattering centres by means of ITP technique.

To further investigate the reliability of the profiles obtained after the proposed CLEAN-based technique, we compare in Fig. 14 the results obtained for test M2 to that of test M1. Specifically Fig. 14(a) and Fig. 14(b) have been obtained by exploiting ISAR CPIs of 6 sec temporally displaced along the available acquisitions of 10 sec; moreover, for a convenient comparison, the CPIs adopted for test M1 have been properly selected so as to guarantee that the car was observed from about the same view angle with respect to the leading car of test M2.

Notice that, in both figures, the corresponding cross-range profiles largely overlap, namely almost the same pattern of
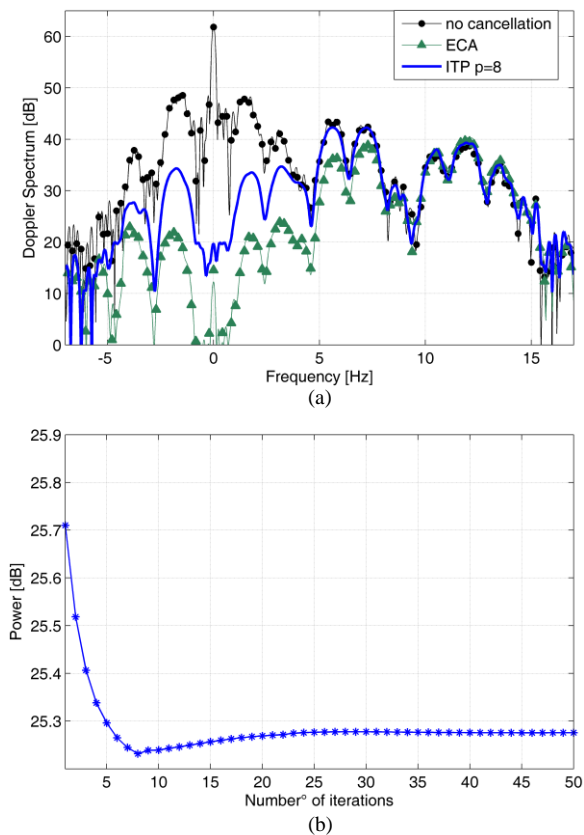

Fig. 12. Experiment M1. (a) Signal Doppler spectrum. (b) Residual power level of the target-free signal at the range bin of interest as a function of the iteration number.
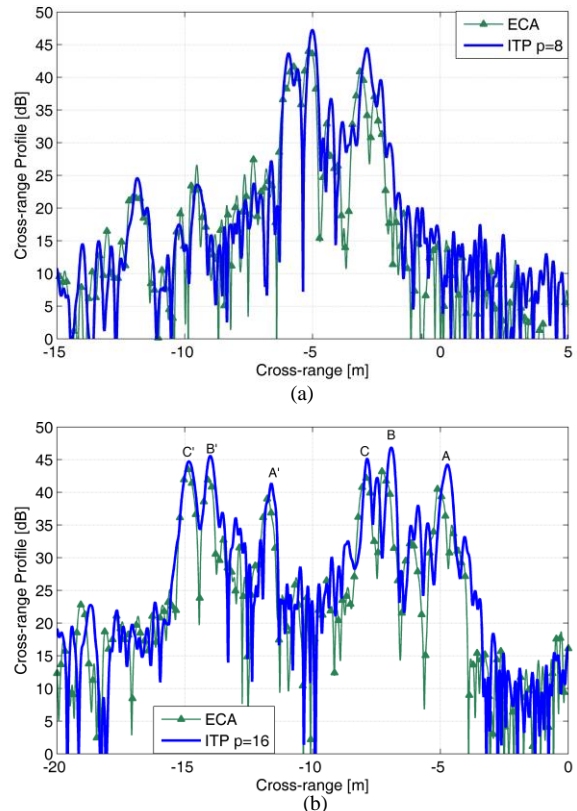

Fig. 13. Cross-range profiles comparison for the real data. (a) Experiment M1. (b) Experiment M2.

dominant scatterers is obtained even if different experiments (M1 and M2) are considered. In addition, by comparing Fig. 14(a) and Fig. 14(b), we might observe that the shape of the profiles has a remarkable temporal stability along the performed acquisition for both test M1 and test M2.

The reported results demonstrate the effectiveness of the proposed experimental setup and processing scheme and support the practical application of the WiFi-based passive ISAR for short range (both indoor/outdoor) surveillance applications. In particular the comparison above clearly shows the reliability and stability of the achieved profiles which might fruitfully feed a classification stage based on appropriate signatures database.

VII. CONCLUSION

In this paper the potentialities of a WiFi-based passive radar have been investigated for indoor area monitoring. In particular, we have demonstrated that it is possible to detect and localize non cooperative moving targets by exploiting Wi-Fi transmission. Additionally, in order to improve the resolution capabilities of the proposed system, suitable ISAR techniques have been introduced to allow the achievement of high resolution cross-range profiles of the detected targets. The required processing chain for detection, localization and profiling has been described: particularly in order to obtain high quality ISAR products in all conditions a new iterative target preserving technique has been proposed suitable for the simultaneous rejection of the background disturbance (stationary scene, multipath, etc etc) and profiling of the target. By using this technique, based on a clean-like approach, reliable ISAR profiles can be obtained even when disturbance and target are largely overlapped in Doppler domain.

The effectiveness of the proposed system and processing techniques has been demonstrated by means of the results obtained for several data sets acquired during experimental campaigns with a setup developed at the University of Rome "La Sapienza".

In particular it has been shown that human targets moving in indoor environment can be detected and accurately localized by exploiting proper multistatic geometries with few receiving antennas. We point out that the few examples reported have been selected, for illustrative purposes, among the experimental tests of a much more extensive campaign performed by the authors during the demonstration stage of the EU FP7 ATOM project [12]. The results obtained throughout the test campaign are in large agreement with those reported in the paper thus demonstrating that the WiFi-based PCL sensor can be successfully employed (with other active and passive radar sensors) for detecting and tracking suspicious people within the Terminal area of the airport.

The application of ISAR techniques against the echoes from human targets moving indoor clearly show the improved resolution capabilities which could enable the separation of closely spaced targets, otherwise not separable. Moreover reliable and stable profiles of moving man-made objects are achieved with a cross-range resolution up to about 10 cm. This has been shown in this paper with reference to an experimental

TABLE II
CROSS-RANGE DISPLACEMENTS OF HOMOLOGOUS POINTS OF THE PROFILES
OBTAINED FOR TEST M2

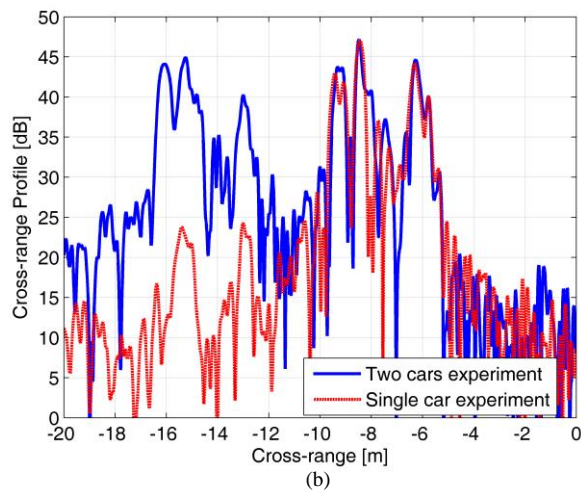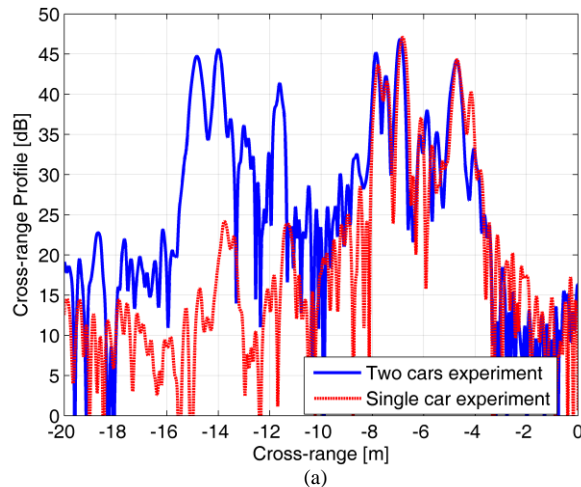|	ECA	ITP (iter p=16)
$D_A = |A'-A|$	6.67 m	6.88 m
$D_B = |B'-B|$	6.84 m	7.08 m
$D_C = |C'-C|$	7.03 m	6.97 m

(a)

(b)

Fig. 14. Profiles comparison between test M1 (single car) and test M2 (two cars) for two different selected CPI.

test including two identical cars (i.e. Fiat Punto Evo). Moreover similar results have been obtained against different tests where different cars models were employed with the same acquisition geometry. This allowed us to preliminary verify that these profiles could be exploited for classification purposes.

The results shown support the practical applicability of the WiFi-based passive radar concept for improving internal and external security of private/public premises and demonstrate its suitability to be usefully employed in an integrated multi-sensor surveillance system.

REFERENCES

[1] T. Sanpechuda and L. Kovavisaruch, "A review of RFID localization: Applications and techniques," in *Proc. IEEE Int. Conf. Electr.Eng./Electron. Comput. Telecommun. Inf. Technol.*, May 2008, pp. 769–772.

[2] H. Liu, H. Darabi, P. Banerjee, and L. Jing, "Survey of Wireless Indoor Positioning Techniques and Systems," *IEEE Transactions on Systems, Man, and Cybernetics, Part C: Applications and Reviews,* vol.37, no.6, pp.1067–1080, Nov. 2007.

[3] A. Athalye, V. Savic, M. Bolic, and P.M. Djuric, "Novel Semi-Passive RFID System for Indoor Localization," *IEEE Sensors Journal,* vol.13, no.2, pp.528–537, Feb. 2013.

[4] D. Dardari, R. D'Errico, C. Roblin, A. Sibille, and M.Z. Win, "Ultrawide Bandwidth RFID: The Next Generation?," in *Proc. IEEE* , vol.98, no.9, Sept. 2010.

[5] P. Howland, "Special Issue on Passive Radar Systems," *IEE Proceedings on Radar, Sonar and Navigation*, Vol. 152, Issue 3, June 2005.

[6] Special Issue on Passive Radar – *IEEE Aerospace and Electronic Systems Magazine*, Vol. 27, Issue 10, October 2012.

[7] F. Colone, K. Woodbridge, H. Guo, D. Mason, and C.J. Baker, "Ambiguity Function Analysis of Wireless LAN Transmissions for Passive Radar," *IEEE Transactions on Aerospace and Electronic Systems*, January 2011, 47, (1), pp. 240-264.

[8] P. Falcone, F. Colone, and P. Lombardo, "Potentialities and challenges of WiFi-based passive radar," *IEEE Aerospace and Electronic Systems Magazine*, November 2012, 27, (11), pp. 15-26.

[9] F. Colone, P. Falcone, C. Bongioanni, and P. Lombardo, "WiFi-Based Passive Bistatic Radar: Data Processing Schemes and Experimental Results," *IEEE Transactions on Aerospace and Electronic Systems*, April 2012, 48, (2), pp. 1061-1079.

[10] P. Falcone, F. Colone, A. Macera, and P. Lombardo, "2D Location of Moving Targets within Local Areas using WiFi-based Multistatic Passive Radar," *IET Radar Sonar and Navigation*, vol.8, no.2, pp. 123-131, February 2014.

[11] K. Chetty, G.E. Smith, and K. Woodbridge, "Through-the-Wall Sensing of Personnel Using Passive Bistatic WiFi Radar at Standoff Distances," *IEEE Transactions on Geoscience and Remote Sensing*, April 2012, 50, (4), pp. 1218-1226.

[12] FP7-AAT-2007-RTD-1: ATOM - "Airport detection and Tracking Of dangerous Materials by passive and active sensors arrays", project funded by the European Union, 7th Framework Program, Theme #7 Transport (including Aeronautics), Grant Agreement No.: 218041, http://www.atom-project.eu.

[13] FP7-PEOPLE-2011-IAPP: SOS - "Sensors system for detection and tracking Of dangerous materials in order to increase the airport Security in the indoor landside area", project funded by the European Union, 7th Framework Program, Marie Curie Action, Grant Agreement No.: 286105, http://www.sos-project.eu.

[14] F. Colone, D. Pastina, P. Falcone, and P. Lombardo, "WiFi-based passive ISAR for high resolution cross-range profiling of moving targets," *IEEE Transactions on Geoscience and Remote Sensing*, vol. 52, no. 6, pp. 3486-3501, June 2014.

[15] D.R. Wehner, *High-Resolution Radar*, 2nd edition, Boston, MA, USA: Artech House, 1995, Ch. 7, pp.341-364.

[16] F. Colone, P. Falcone, and P. Lombardo, "Passive Bistatic Radar based on mixed DSSS and OFDM WiFi transmissions," in *Proc. 2011 European Radar Conference*, Manchester, U.K., October 2011, pp. 154-157.

[17] F. Colone, D.W. O'Hagan, P. Lombardo, and C.J. Baker, "A Multistage Processing Algorithm for Disturbance Removal and Target Detection in Passive Bistatic Radar," *IEEE Transactions on Aerospace and Electronic Systems*, April 2009, 45, (2), pp. 698-722.

[18] P. Falcone, F. Colone, and P. Lombardo, "Doppler Frequency Sidelobes Level Control for WiFi-Based Passive Bistatic Radar," in *Proc. 2011 IEEE Radar Conference,* Kansas City, MO, USA, May 2011, pp. 435-440.

[19] A. Macera, C. Bongioanni, F. Colone, and P. Lombardo, "Receiver architecture for multi-standard based Passive Bistatic Radar," in *Proc. 2013 IEEE Radar Conference*, Ottawa, Ontario, Canada, 29 April-3 May 2013.

[20] K. S. Kulpa and Z. Czekala, "Masking effect and its removal in PCL radar," *Proc. Inst. Elect. Eng.—Radar, Sonar Navig.*, vol. 152, no. 3, pp. 174–178, Jun. 2005.

[21] T. Jenho and B.D. Steiberg, "Reduction of sidelobe and speckle artifacts in microwave imaging: the CLEAN technique," *IEEE Transactions on Antennas and Propagation*, Vol. 36, Issue 4, 1988, pp.543-556.

Debora Pastina (M'01) received the Laurea degree in telecommunications engineering and the Ph.D. degree in information and telecommunications engineering from the University of Rome "La Sapienza," Rome, Italy, in 1996 and 2000, respectively.

From July 1998 to March 1999, she carried on research activity with the SAR Processing Team, Defence Evaluation Research Agency (DERA), Malvern, U.K. She is currently an Assistant Professor with the DIET Department, University of Rome "La Sapienza," where she teaches different courses in remote sensing and telecommunication. She is involved, and is responsible of, scientific research projects funded by the Italian Ministry of Research, by the Italian Space Agency, by the European Commission and by the national radar industry. Her main research interests include SAR/ISAR signal processing, GMTI techniques, clutter models, coherent and incoherent radar detection in non-Gaussian clutter and CFAR radar techniques. The results of her research activity have been reported in a number of journal and conference papers.

Dr. Pastina was the Chairman of the Local Committee of the IEEE/ISPRS Joint Workshop on Remote Sensing and Data Fusion over Urban Areas (Rome, November 2001). She was the Publication Chair of the 2008 IEEE Radar Conference held in Rome in May 2008. She has been a member of the Editorial Board of the International Journal of Electronics and Communications (AEÜ, Elsevier) acting as Area Editor for radar systems and techniques since September 2012. She has served in the technical review committee of many international conferences on radar systems and remote sensing. From many years she is frequently reviewer for a number of international technical journals.

Fabiola Colone (S'02–M'06) received the laurea degree in communication engineering and the Ph.D. degree in remote sensing from the University of Rome "La Sapienza", Rome, Italy, in 2002 and 2006, respectively.

She joined the INFOCOM Dept., University of Rome "La Sapienza", Italy, as a Research Associate in January 2006. From December 2006 to June 2007, she was a Visiting Scientist at the Electronic and Electrical Engineering Dept. of the University College London,

London, U.K. She is currently an Assistant Professor at the DIET Department of the University of Rome "La Sapienza".

Her current research interests include passive coherent location (PCL), multi-channel adaptive signal processing, and space-time adaptive processing (STAP) with application to mono- and bi-static radar systems. She is involved in scientific research projects funded by the European Union, the Italian Space Agency, the Italian Ministry of Research, and the Italian Industry.

Dr. Colone's research has been reported in over 70 publications in international technical journals and conference proceedings. She was in the organizing committee, as the Student Forum Co-Chair, of the IEEE 2008 Radar Conference, Rome, Italy. From 2010 she is member of the Editorial Board of the International Journal of Electronics and Communications (AEÜ) (Elsevier). She served in the technical committee of many international conferences on radar systems and signal processing, and she is frequently reviewer for a number of international technical journals.

Tatiana Martelli received the Master degree 'cum laude' in Communication Engineering from "La Sapienza" University of Rome, Rome, Italy, in 2012, where she is currently a third year Ph.D. student in remote sensing.

Her research interests include passive radar systems; in particular, she works on the design of signal processing techniques for detection, localization and imaging of targets within short-medium range. She is involved in SOS project funded by the European Union.
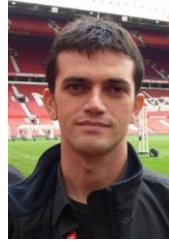
Paolo Falcone received the Laurea degree in telecommunications engineering and the Ph.D. degree in remote sensing from the University of Rome "La Sapienza", Rome, Italy, in 2008 and 2013, respectively.

His research was about signal processing for passive radar systems. Since 2012 he is R&D Engineer at the electronic developments dept. of ARESYS srl, a spin-off of Politecnico di Milano.